MODELING THE LIGHT DIFFRACTION BY MICRO-OPTICS ELEMENTS USING THE FINITE ELEMENT METHOD

*D. V. Nesterenko, V.V. Kotlyar, Y.Wang**
Image Processing Systems Institute of Russian Academy of Sciences, Russia
**) Beijing Institute of Technology, Beijing 100081, China*

1. Introduction

Technological advances made possible micro-processing of optical and diffractive devices of sub-wavelength size. Such elements may find use in holography, spectroscopy, interferometry, and optical data processing.

The rigorous modeling of these devices calls for solving the basic electromagnetic Maxwell's equations. If one needs to get a far-field solution, commonly used geometrical optics approximations become inadequate, which entails the necessity of developing numerical techniques for solving Maxwell's equations. For a sub-wavelength characteristic size of diffractive structures, one should use a vector model for analyzing diffraction processes [1]. The vector diffraction problem may be solved analytically for some periodic structures [2]. Hence, the vector diffraction by a periodic diffractive optical elements (DOEs) should be simulated using numerical techniques. These numerical techniques may then be used in working out recommendations how to improve the parameters of fabricated devices or to optimize the process of developing new ones.

The majority of numerical diffraction models aimed at analyzing conducting electromagnetic scatters may be divided into differential [3], integral, and variational.

With integral methods, the electromagnetic field at a space point is found as a combination of contributions to this point from source fields, taken over space or surface. Popularity of the integral methods is due to their ability to deal with unlimited field problems since the Zommerfeld radiation condition holds unconditionally in the problem statement. Furthermore, the integral methods require that only the surface field of a diffraction element be known, and not the total spatial field, thus minimizing the number of unknowns. A disadvantage of the integral methods is that they lead to fully completed matrixes and, hence, require large bulk of computer memory and great computational efforts. Note that volume integral methods are also able to simulate diffraction by nonhomogeneous DOEs.

Variational methods applied to solving limit-volume tasks find the solution to Helmholtz's equation by minimizing the functional relation, as opposed to directly solving differential equations. If the finite element method is stated using the Ritz- method, it is represented by a variational approximation. Its statement is simple and apply to an arbitrary homogeneous medium. However, it involves no Zommerfeld radiation condition. It is common practice to use an absorbing boundary condition which is also not free from disadvantages.

There is also a hybrid method [1] which implies the application of the finite element method (FEM) to the internal DOE region where nonhomogeneities may occur, and the application of the boundary element method to a DOE-external region, with the radiation conditions to be fulfilled. The methods meet on the interface, thus satisfying the field continuity condition. This approximation represents a faithful boundary condition since values of the normal derivative of reflected field are given exactly. A disadvantage of the method lies in the nondiagonal character of the matrix system, which leads to a completely filled submatrix resulting in a greater memory resources for data storage and great computational efforts.

2. Statement of the problem

It has been known that for a nonhomogeneous, slow-varying (as compared with the wavelength) medium the set of Maxwell's equations may be reduced to the Helmholtz equation for each component of the electric and magnetic vectors [4].

The boundary Γ envelops the space region with scattering microstructure, and a free space domain . The internal domain is designated I, the internal domain I with its boundary Γ is designated Ω. The external domain Ψ with respect to Γ is supposed to be unlimited free space.

The element (diffractive device, DOE) stretches infinitely along the z axis, whereas its cross-section is found in the xy. So, the resulting solution is z-independent, but depends only on the x- and y-variables. Any such 2D task may be expanded into transverse magnetic TM-polarization and transverse electric TE-polarization.

Let us consider TM-and TE-polarization independently, which enables each projection of the electromagnetic field to be described by one scalar function $u(x, y)$. For TM-polarization $u(x, y)$ is the total electric field $E_z(x, y)$, and for TE-polarization $u(x, y)$ is the total magnetic field $H_z(x, y)$. In either case, the total field $u(x, y)$ is represented by the sum of scattered field $u^{sc}(x,y)$ and incident field $u^{inc}(x, y)$.

The total field $u_\Omega(x, y)$ in Ω should satisfy the Helmholtz equation:

$$\nabla \cdot \left[\frac{1}{p} \nabla u_\Omega(x, y) \right] + k_0^2 q u_\Omega(x, y) = 0 , \qquad (1)$$

where $p=\mu_r$ and $q=\varepsilon_r$ for TM-polarization, and $p=\varepsilon_r$ and $q=\mu_r$ for TE-polarization. The constants μ_r and ε_r are defined by the ratio of magnetic permeability and electric permittivity of a uniform medium to the analogous free space parameters, i.e. $\mu_r=\mu/\mu_0$ and $\varepsilon_r=\varepsilon_r/\varepsilon_0$, k_0 is the wavenumber in free space.

3. The Ritz method

To solve the problem in Eq. (1) consider the functional:

$$\mathrm{J(u)=(Lu,u) - 2(f,u)} = \iint_\Omega \left(- u(\Delta u) - qpk^2 u^2 \right) \mathrm{dxdy}. \qquad (2)$$

Using the first Green formula

$$\iint_{\Omega} P\Delta Q \, d\Omega = \int_{\Gamma} P \frac{dQ}{d\mathbf{n}'} dl - \iint_{\Omega} \nabla P \nabla Q \, d\Omega, \quad (3)$$

where Ω – is the domain of the plane x, y; Γ – is its boundary went around in positive direction; $\frac{dQ}{d\mathbf{n}'}$ – is the derivative in the direction of the external normal to the curve Γ, instead of Eq. (2) we get:

$$J(u) = \iint_{\Omega} \left(\nabla u \nabla u - qpk^2 u^2 \right) dxdy - \int_{\Gamma} u \frac{du}{d\mathbf{n}'} dl. \quad (4)$$

Since the incident field $u^{inc}(x,y)$ is known Eq. (1) should be resolved relative to the scattered field $u^{sc}(x,y)$. Instead of Eq. (4) for the sum of scattered and incident fields we get the following functional:

$$J[u^{sc}_{\Omega}(x,y)] = \iint_{\Omega} \left\{ \frac{1}{p(x,y)} \nabla u^{sc}_{\Omega}(x,y) \cdot \nabla u^{sc}_{\Omega}(x,y) - k_0^2 q(x,y) \left[u^{sc}_{\Omega}(x,y) \right]^2 \right\} d\Omega +$$

$$+ 2 \iint_{\Omega} \left\{ \frac{1}{p(x,y)} \nabla u^{sc}_{\Omega}(x,y) \cdot \nabla u^{inc}_{\Omega}(x,y) - k_0^2 q(x,y) u^{sc}_{\Omega}(x,y) \cdot u^{inc}_{\Omega}(x,y) \right\} d\Omega -$$

$$- \oint_{\Gamma} u^{sc}_{\Omega}(x,y) \left[\frac{\partial u^{sc}_{\Omega}(x,y)}{\partial \mathrm{n}'} + \frac{\partial u^{inc}_{\Omega}(x,y)}{\partial \mathrm{n}'} \right] dl + \text{Const.} \quad (5)$$

We seek the extremum of the functional J:

$$\delta J[u^{sc}_{\Omega}(x,y)] = 0. \quad (6)$$

Reduce Eq. (6) to a set of linear algebraic equations using the following scheme. Cover the domain Ω by a triangle network, with a linear polynomial constructed in each triangle. For a unique definition of the polynomials it will suffice to specify their values at the triangles' vertices. Thus, the system of functions $\omega_k(x, y)$ will form the basis. The $\omega_k(x, y)$ function is represented geometrically as a pyramid with the center at point C_k (Fig. 1).

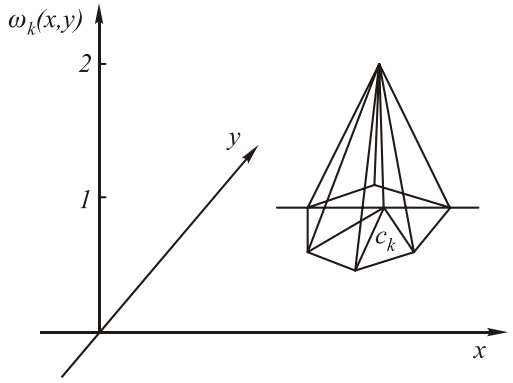

Fig. 1. Geometrical representation of the $\omega_k(x, y)$ *function*

The domain Ω will be represented by $2(\sqrt{N}-1)^2$ triangular elements, while the domain Γ will be represented by $M = 4(N-1)$ linear segments, where N – is the number of nodes of the network. The field u is represented via this basis as follows

$$u(x, y) = \sum_{k=1}^{N} u_k \omega_k^{\Omega}(x, y). \quad (7)$$

Substituting the expansion in Eq. (7) into the functional in Eq. (5), making the derivatives $\partial J(u)/\partial u_k$ (k=1, …, N) be equal to zero and separating the total field into the sum of incident and scattered fields, we get the following set of linear algebraic equations:

$$\mathbf{A}(u^{sc} + u^{inc}) - \frac{1}{2}\mathbf{B}(v^{sc} + v^{inc}) = 0. \quad (8)$$

The elements of matrix **A** are derived from:

$$a_{k,j} = \iint_{\Omega_k} \left(\frac{1}{p(x,y)} \left[\frac{\partial \omega_k^{\Omega}(x,y)}{\partial x} \frac{\partial \omega_j^{\Omega}(x,y)}{\partial x} + \right. \right.$$
$$\left. \left. + \frac{\partial \omega_k^{\Omega}(x,y)}{\partial y} \frac{\partial \omega_j^{\Omega}(x,y)}{\partial y} \right] - k_0^2 q(x,y) \omega_k^{\Omega}(x,y) \omega_j^{\Omega}(x,y) \right) d\Omega, \quad (9)$$

k, j = 1, ..., N.

The matrix **B** elements are derived from:

$$b_{m,s} = \oint_{\Gamma} \omega_m^{\Gamma} \omega_s^{\Gamma} \, dl, \; m, s = 1, ..., M. \quad (10)$$

Then, for Eq. (8) we get:

$$\begin{bmatrix} \mathbf{A}_{I,I} & \mathbf{A}_{\Gamma,I} & 0 \\ \mathbf{A}_{I,\Gamma} & \mathbf{A}_{\Gamma,\Gamma} & \mathbf{B} \end{bmatrix} \begin{bmatrix} \bar{\mathbf{u}}_I^{sc} \\ \bar{\mathbf{u}}_{\Gamma}^{sc} \\ \bar{\mathbf{v}}_{\Gamma}^{sc} \end{bmatrix} =$$

$$- \begin{bmatrix} \mathbf{A}_{I,I} & \mathbf{A}_{\Gamma,I} & 0 \\ \mathbf{A}_{I,\Gamma} & \mathbf{A}_{\Gamma,\Gamma} & \mathbf{B} \end{bmatrix} \begin{bmatrix} \bar{\mathbf{u}}_I^{inc} \\ \bar{\mathbf{u}}_{\Gamma}^{inc} \\ \bar{\mathbf{v}}_{\Gamma}^{inc} \end{bmatrix}. \quad (11)$$

In Eq. (11), the between-field relation coefficients only in the internal nodes are represented by the submatrix $(N-M)\times(N-M)$ $[\mathbf{A}_{I,I}]$. . The between-field relation coefficients only on the boundary nodes are given by the submatrix $M\times M$ $[\mathbf{A}_{\Gamma,\Gamma}]$, while the between-field relations on internal and boundary nodes is given by the submatrix $(N-M)\times M$ $[\mathbf{A}_{\Gamma,I}]$ and the transposed matrix $[\mathbf{A}_{I,\Gamma}]$. The interaction between derivatives of the field variables on the boundary nodes is represented by the submatrix $M\times M$ [**B**].

In the set, the number of equations is less than the number of unknowns, thus making it necessary to specify either the normal field derivative on the interface or the field value. In this paper we develop a boundary element method (BEM) that defines the relation between the fields and their derivatives on the boundary.

As an alternative, one may determine the field in I, using integration machinery. Analysis of homogeneous DOEs using the boundary integral technique applied to its natural boundary is made in Ref. [1]. On the other

hand, an imaginary boundary can reduce the number of linear segments involved in the boundary description, but simultaneously results in the generation of an arbitrary nonhomogeneous scatterer that denies analyzing by means of the boundary integral method. Note that although the volume integration techniques allow the nonhomogeneous scatterers to be analyzed, the FEM requires less computational efforts.

4. Results of numerical simulation

The above-described algorithm was applied for computation of the diffraction light field from a desired-shape DOE.

Functions $\cos(k_0 nx)$ and $\sin(k_0 nx)$ are known to be solutions of Eq. (1), where k_0 is the wavevector of free space and n is the refractive index of medium.

For the Dirichlet problem ($u^{sc} = 0$) attacked by the Gauss method, the linear set of algebraic equations is given by

$$\left[\left[\mathbf{A}_{I,I}\right]\ \left[\mathbf{A}_{\Gamma,I}\right]\right]\begin{bmatrix}\bar{\mathbf{u}}_I\\ \bar{\mathbf{u}}_\Gamma\end{bmatrix} = [0] \qquad (12)$$

or

$$\left[\mathbf{A}_{I,I}\right]\left[\bar{\mathbf{u}}_I\right] = -\left[\mathbf{A}_{\Gamma,I}\right]\left[\bar{\mathbf{u}}_\Gamma\right]. \qquad (13)$$

Assuming $\bar{\mathbf{u}}_\Gamma$ being equal to the values the sine or cosine function take on the boundary Γ, we should get $\bar{\mathbf{u}}_I$ being equal to the values the sine or cosine functions take in the internal domain I. In all cases, a plane incident wave moves from the left. Three sets of computation were conducted with various values of the sampling parameter N (the number of break-down points). The size of the estimated domain and the wavelength were, respectively, $S = 4.225$ μm and $\lambda = 1.3$ μm. Throughout the entire estimated domain, we assumed the magnetic permeability $\mu = 1$, the dielectric constant $\varepsilon = 1$ and the refractive index $n = 1$.

In the first set, the real part of $\bar{\mathbf{u}}_\Gamma$ was described by the function $\cos(k_0 nx)$, with its argument belonging to the boundary Γ, and complex part was taken to equal zero. The function $\cos(k_0 nx)$ is also a solution of the task with the above boundary conditions. Figure 2 shows the intensity distribution for the field $\bar{\mathbf{u}}_\Omega$ and the intensity distribution over the cross-section $y = 1.2$ μm. The sampling step is $N = 75$x75. In terms of intensity δ_I, the root-mean-square deviation of the generated field from the field $\cos(k_0 nx)$ was 7 %. In terms of amplitude, the r.m.s. deviation was 4 %.

In the second case, the real part of $\bar{\mathbf{u}}_\Gamma$ was described by the $\sin(k_0 nx)$ function, with its argument belonging to the boundary Γ and complex part being equalled to zero. The solution of the problem with the above-described boundary conditions is the $\sin(k_0 nx)$ function. In the third case, the propagation of a plane wave was computed. The real part $\bar{\mathbf{u}}_\Gamma$ was described by the $\cos(k_0 nx)$ function, while the complex part was described by the $\sin(k_0 nx)$ function, with their argument belonging to the boundary Γ. The solution of the problem with such boundary conditions is given by the $\exp(ik_0 nx)$ function.

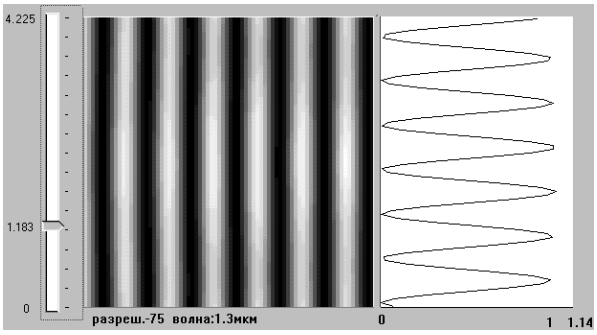

Fig. 2. Intensity distribution for the Dirichlet problem at $\bar{\mathbf{u}}_\Gamma^{inc}$ *equal to cos(*$k_0$nx*)*

The plot in Fig. 3 shows how the root-mean-square deviation of intensity depends on the $Z = \sqrt{N}$ parameter for the size of the domain under calculation S =4.225 μm and the wavelength 1.3 μm.

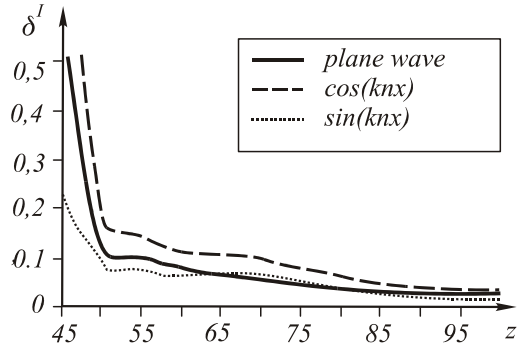

Fig. 3. Root-mean-square intensity deviation δ_I *vs the* $Z = \sqrt{N}$ *parameter*

For the Neumann task ($v^{sc} = 0$) solved by use of the Gauss method, the sets of equations are given by

$$\begin{bmatrix}\left[\mathbf{A}_{I,I}\right] & \left[\mathbf{A}_{\Gamma,I}\right] & 0\\ \left[\mathbf{A}_{I,\Gamma}\right] & \left[\mathbf{A}_{\Gamma,\Gamma}\right] & [\mathbf{B}]\end{bmatrix}\begin{bmatrix}\bar{\mathbf{u}}_I\\ \bar{\mathbf{u}}_\Gamma\\ \bar{\mathbf{v}}_\Gamma\end{bmatrix} = [0] \qquad (14)$$

or

$$\begin{bmatrix}\left[\mathbf{A}_{I,I}\right] & \left[\mathbf{A}_{\Gamma,I}\right]\\ \left[\mathbf{A}_{I,\Gamma}\right] & \left[\mathbf{A}_{\Gamma,\Gamma}\right]\end{bmatrix}\begin{bmatrix}\bar{\mathbf{u}}_I\\ \bar{\mathbf{u}}_\Gamma\end{bmatrix} = -[\mathbf{B}]\left[\bar{\mathbf{v}}_\Gamma\right]. \qquad (15)$$

In all situations, a plane incident wave travels from the left.

We considered how a TM-polarized wave of wavelength 1.3 μm traveled in a homogeneous medium of lens with permittivity $\mu = 1$ and dielectric permeability $\varepsilon = 1$.

Figure 4 depicts the result of numerical simulation for a lens of radius $R = 2$ μm (thickness 2 μm), aperture 4 μm, focal length 4 μm. The refractive index is $n = 1.5$ and focal length is $f = 4$ μm. Size of the domain to be calculated is $S = 7.7$ x 7.7 μm. The lens is 0.6 μm apart from the left edge. The sampling parameter is $N = 115$ x 115. The boundary conditions were given by the field normal derivative on the boundary, equal to the derivative of the $\exp(ik_0 x)$ function, i. e. the field derivatives

are not equal to zero on the left and right boundary and are equal to zero on the top and bottom boundary. Such boundary conditions correspond to the propagation of the field from left to right along top and bottom boundary. Intensity distributions for lenses of thickness 1.8 μm and 1.7 μm, respectively, are depicted in Figs. 5 and 6.

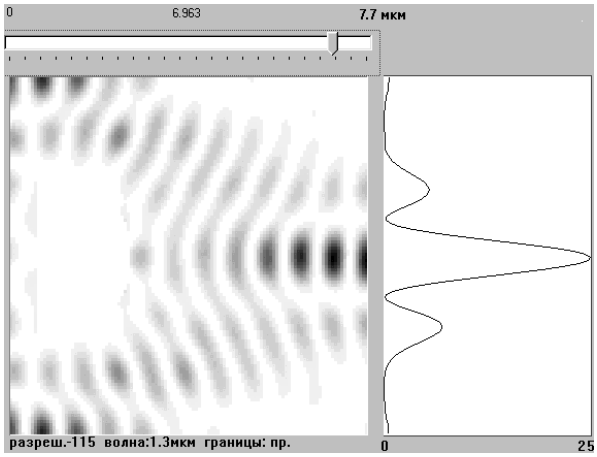

Fig. 4. Intensity distribution (inverted) for the Neumann task at n *= 1.5.*

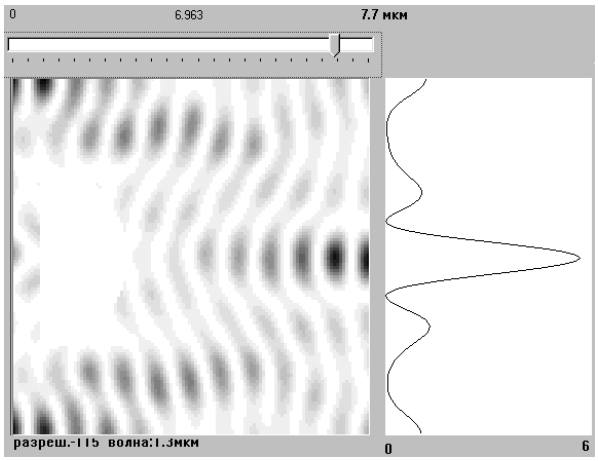

Fig. 5. Intensity distribution (inverted) for a lens of thickness 1.8 μm.

From Fig. 5, the lens is seen to bend the wavefront making it spherical. The field solution is constructed so that that the derivatives on the top and bottom boundaries are equal to zero and diffraction lines are perpendicular to these boundaries. A maximum intensity is observed in the proposed focus.

5. Conclusion

For analysis of vector diffraction by microstructures, the Ritz method has been developed. The effect of focusing of a plane wave of wavelength 1.3 μm by a lens of radius 2 μm, aperture 2 μm and focal length 4 μm has been clearly demonstrated. The algorithms developed make it possible to derive the approximate solution of desired accuracy not at the cost of an increases network step, but through constructing of more accurate approximations of the initial problem. as continuation of the work, the analysis of light propagation and diffraction in free space may be conducted.

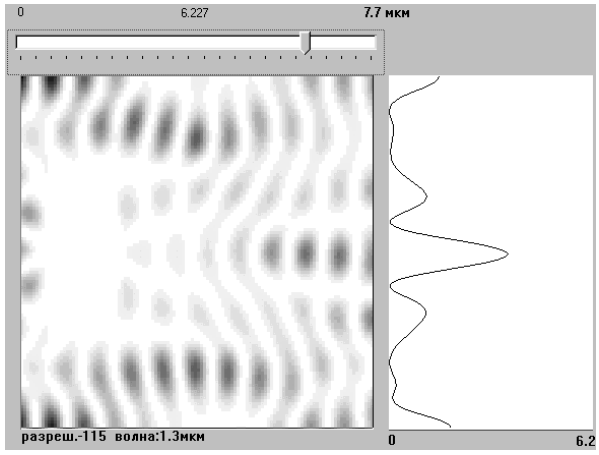

Fig. 6. Intensity distribution for a lens of thickness 1.7 μm

6. Acknowledgment

This work was supported by the Russian Foundation for Basis Research (grants 98-01-00894, 99-01-39012).

7. References

1. Mirotznik M.S., Prather D.W., Mait J.N. A hybrid finite element – boundary element method for the analysis of diffractive elements.//Journal Of Modern Optics.-1996.-v.43.-no.7.-p.1309.
2. B. Lichtenberg, Gallagher N.C. Numerical modeling of diffractive devices using the finite element method.//Optical Engineering. -Nov.1994.-v.33.-no.11.-p.3518.
3. D. L. Golovashkin, A. A. Degtyarev, V. A. Soifer, Modeling the waveguide optical radiation propagation using the electromagnetic theory, Journal of Computer Optics, 1997, No. 17, p. 5.
4. S. Solimeno, B. Crosiniani, P. Di Porto, diffraction and wavegiude propagation of optical radiation, Moscow, Mir Publishers, 1984, p. 13, 256 pages.
5. G. I. Marchuk, Methods of computational mathematics, Moscow, Mir Publishers, 1980, p. 32, p.64.

Modeling the light diffraction by micro-optics elements using the finite element method

D.V. Nesterenko, V.V. Kotlyar, Y.Wang[1]
Image Processing Systems Institute of Russian Academy of Sciences, Russia
[1]*Beijing Institute of Technology, Beijing 100081, China*

Abstract

Technological advances has made it possible to perform microprocessing of optical and diffractive devices of subwavelength size. Such elements can be applied in holography, spectroscopy, interferometry, and optical data processing.

Citation: Nesterenko DV, Kotlyar VV, Wang Y. Modeling the light diffraction by micro-optics elements using the finite element method. Computer Optics 1999; 19: 40 - 43.

References

[1] Mirotznik M.S., Prather D.W., Mait J.N. A hybrid finite element – boundary element method for the analysis of diffractive elements.//Journal Of Modern Optics.-1996.-v.43.-no.7.-p.1309.
[2] B. Lichtenberg, Gallagher N.C. Numerical modeling of diffractive devices using the finite element method.//Optical Engineering. -Nov.1994.-v.33.-no.11.-p.3518.
[3] D. L. Golovashkin, A. A. Degtyarev, V. A. Soifer, Modeling the waveguide optical radiation propagation using the electromagnetic theory, Journal of Computer Optics, 1997, No. 17, p. 5.
[4] S. Solimeno, B. Crosiniani, P. Di Porto, diffraction and wavegiude propagation of optical radiation, Moscow, Mir Publishers, 1984, p. 13, 256 pages.
[5] G. I. Marchuk, Methods of computational mathematics, Moscow, Mir Publishers, 1980, p. 32, p.64.